J|A|C|S
COMMUNICATIONS

# Solid-State $^{55}$Mn NMR Spectroscopy of Bis($\mu$-oxo)dimanganese(IV) [$Mn_2O_2$(salpn)$_2$], a Model for the Oxygen Evolving Complex in Photosystem II

Paul D. Ellis,[†] Jesse A. Sears,[‡] Ping Yang,*[,‡] Michel Dupuis,[§] Thaddeus T. Boron III,[||] Vincent L. Pecoraro,[||] Troy A. Stich,[⊥] R. David Britt,[⊥] and Andrew S. Lipton*[,†]

*Biological Sciences Division, Environmental Molecular Sciences Laboratory, and Chemical and Material Sciences Division, Pacific Northwest National Laboratory, 902 Battlelle Boulevard, Richland, Washington 99352, United States, Department of Chemistry, University of Michigan, 930 North University Avenue, Ann Arbor, Michigan 48109-1055, United States, and Department of Chemistry, University of California—Davis, One Shields Avenue, Davis, California 95616, United States*

Received June 30, 2010; E-mail: ping.yang@pnl.gov; as.lipton@pnl.gov

***Abstract:*** We have examined the antiferromagneticly coupled bis($\mu$-oxo)dimanganese(IV) complex [$Mn_2O_2$(salpn)$_2$] (**1**) with $^{55}$Mn solid-state NMR at cryogenic temperatures and first-principle theory. The extracted values of the $^{55}$Mn quadrupole coupling constant, $C_Q$, and its asymmetry parameter, $\eta_Q$, for **1** are 24.7 MHz and 0.43, respectively. Further, there was a large anisotropic contribution to the shielding of each $Mn^{4+}$, i.e. a $\Delta\sigma$ of 3375 ppm. Utilizing broken symmetry density functional theory, the predicted values of the electric field gradient (EFG) or equivalently the $C_Q$ and $\eta_Q$ at ZORA, PBE QZ4P all electron level of theory are 23.4 MHz and 0.68, respectively, in good agreement with experimental observations.

Given the global energy needs, many have sought to understand the details of photosynthesis—in particular, the water splitting reaction—to inspire the development of synthetic energy-producing photocatalysts.[1−6] While the scientific community has made great strides toward this goal, it has fallen short at a critical stage: accurate modeling of the oxygen evolving complex (OEC) found within photosystem II (PSII). Despite the advent of X-ray structures of PSII,[7] the most reliable data we have for the structure of the $Mn_4Ca$ cluster in the OEC come from electron paramagnetic resonance (EPR) and extended X-ray absorption fine structure measurements.[8−11] The resulting magnetic parameters and internuclear distances are critical in constraining theoretical models of the OEC.[12,13] Nonetheless, a consensus on the precise geometry of the $Mn_4Ca$ cluster has yet to be reached. Determining additional spectroscopic properties of the OEC will be of great value in evaluating such computations.

Throughout the S-states of the Kok cycle,[14] the exchange-coupled Mn ions of the OEC are in either the 4+ or 3+ oxidation state. For example, X-ray absorption and EPR studies of PSII in the $S_0$ state suggest the cluster is composed of three Mn(III) ions (each is high-spin $S = 2$) and one Mn(IV) ion ($S = 3/2$) that couple to yield a net $S = 1/2$ spin system.[9,10] As the OEC progresses from $S_0$ through the different S-states, the oxidation state and ligand environment of each metal center can change. The chemical shift tensor ($\sigma$) and electric field gradient (EFG), represented by the quadrupole coupling constant $C_Q$ and the asymmetry parameter ($\eta_Q$) across the $I = 5/2$ $^{55}$Mn nucleus, are expected to be very sensitive reporters of such oxidation-induced changes.

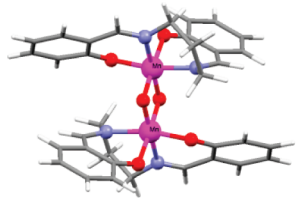

***Figure 1.*** Optimized 3D structure of **1**. The colors denote manganese (magenta), oxygen (red), nitrogen (blue), carbon (gray), and hydrogen (white).

We have previously developed a combined spectroscopic/computational approach to measure and analyze these nuclear quadrupole coupling parameters for metal sites in metalloproteins using cryogenic solid-state nuclear magnetic resonance (NMR) along with density functional theory (DFT) calculations.[15−19] We speculate that such a strategy could be employed to explore potential diamagnetic states of the OEC. As a first step toward this goal, we report the $^{55}$Mn NMR spectrum of the bis($\mu$-oxido)dimanganese(IV) complex [$Mn_2O_2$(salpn)$_2$] (**1**), shown in Figure 1.[20,21] This species is invoked as a model for dimeric Mn(IV) $\mu$-oxo motifs found within the OEC in states $S_1$ through $S_4$.

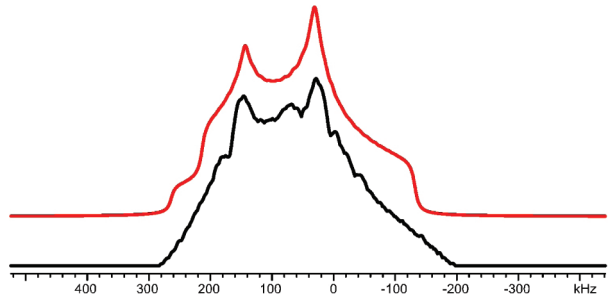


***Figure 2.*** The bottom trace (black) is the experimental NMR spectrum of **1** at 8.5 K. The top trace (red) is the simulation to the experimental data achieved using parameters discussed in the text. Zero frequency occurs at −1162.5 ppm from $MnO_4^{1-}$.

The solid-state NMR spectrum (obtained at 8.5 K and at 9.40 T with a nominal $^{55}$Mn Larmor frequency of 99.019 MHz using the CP/QCPMG pulse sequence[22−24]) of 7 mg of **1** is shown in Figure 2. The spectrum of this Mn(IV)-containing complex is centered halfway between that measured for species with Mn(VII) and Mn(0) oxidation states. For example, $MnO_4^{1-}$ is resonant ca. 0 ppm and

[†] Biological Sciences Division, Pacific Northwest National Laboratory.
[‡] Environmental Molecular Sciences Laboratory, Pacific Northwest National Laboratory.
[§] Chemical and Material Sciences Division, Pacific Northwest National Laboratory.
[||] University of Michigan.
[⊥] University of California—Davis.

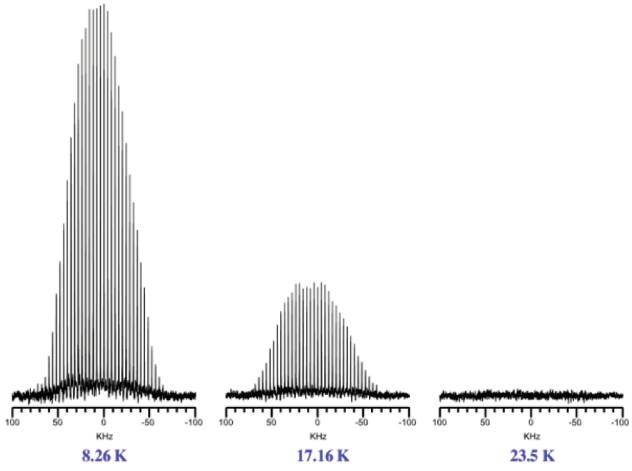


***Figure 3.*** Temperature dependence of the on-resonance portion of the $^{55}$Mn NMR spectrum of **1** acquired at 9.4 T.

$Mn_2(CO)_{10}$ is resonant at −230 kHz (∼ −2325 ppm) to higher shielding or ∼ −1162.5 ppm. Satisfactory simulation of the experimental data presented in Figure 2 was achieved using a single $^{55}$Mn line shape (due to molecular inversion symmetry) with $C_Q$ = 24.7 MHz and $\eta_Q$ = 0.43. The spectral fit required inclusion of a large anisotropic shielding ($\Delta\sigma$ = 3375 ppm) due, most likely, to the concentration of electron density between the two Mn centers, which participates in the exchange interaction and metal-$\mu$-oxo bonding. The value of $\Delta\sigma$ and its appendant Euler angles should be considered approximate until the magnetic field dependence of the lineshape is examined in detail.

Magnetic susceptibility measurements on **1** found the Heisenberg exchange coupling constant[25] to be $J = -92$ cm$^{-1}$ leading to an $S = 0$ ground state.[26] At temperatures below 10 K, $k_BT$ takes on values <7 cm$^{-1}$; thus, the complex does not often sample a paramagnetic excited state (the nearest lying 184 cm$^{-1}$ higher in energy) on the time scale of the experiment. Populating this next electron spin manifold leads to a dramatic broadening of the NMR signal as electron−nuclear spin hyperfine interactions are activated. Indeed, the temperature-dependent intensity of a portion of the $^{55}$Mn NMR spectrum near the on-resonance position of **1** bears out this phenomenon and is presented in Figure 3. The spectrum collected at 17.2 K has approximately 30% of the *S*/*N* of the spectrum obtained at 8.3 K. Increasing the temperature to 23.5 K leads to a complete loss of signal. This behavior implies that just a $2 \times 10^{-5}$% chance of populating a paramagnetic state broadens the NMR spectrum beyond detectable limits. As for the viability of future solid-state NMR studies of antiferromagnetically coupled $S = 0$ species, our findings suggest that the first paramagnetic excited state must be at least 80 cm$^{-1}$ (or a $J$ value of ∼ −40 cm$^{-1}$) away from the ground state to observe appreciable signal intensity (assuming the lowest temperature one can attain routinely in a cryogenic NMR experiment is ∼10 K).

Further insight on the interactions between the metal centers in the Mn(IV,IV) dimer was obtained from density functional theory (DFT). Despite the recent development of computational methods for transition metal NMR calculations,[27−31] the case of multispin site systems including both ferromagnetic and antiferromagnetic systems still remains difficult to handle. Nevertheless, it can be a meaningful starting point to correlate NMR parameters to the general features of electron densities, which can be described reasonably well in a pragmatic way by using the broken symmetry (BS) implementation of DFT.[32,33] A more rigorous study using multiconfigurational electron correlated wave function methods is underway. Computations were performed with the Amsterdam Density Functional program package (ADF).[34−36] All calculations employed the scalar relativistic zeroth-order regular approximation (ZORA)[37,38] within the generalized gradient approximation of the Perdew−Burke−Ernzerhof (PBE) functional for the exchange and correlation potential.[39,40] The geometric structure is optimized using double-ζ Slater-type basis DZP optimized for ZORA calculations (ZORA/DZP) and is found to be in excellent agreement with the experimental values. The computed values for various bond distances and a bond angle are summarized in Table 1 along with the experimental data.

***Table 1.*** Calculated Structural Data and Experimental Measurements Obtained from Crystal Structures

| | Calcd | Expt |
|---|---|---|
| $R$(Mn−Mn) | 2.749 | 2.728 |
| $R$(Mn−$O_{oxo}$) | 1.817 | 1.816 |
| | 1.832 | 1.822 |
| $R$(Mn−$O_{ligand}$) | 1.960 | 1.903 |
| | 1.978 | 1.929 |
| $R$(Mn−N) | 2.032 | 2.013 |
| | 2.088 | 2.065 |
| ∠(Mn−O−Mn) | 97.7° | 97.2° |

The electric field gradients (EFGs) at the metal centers are calculated using the valence quadruple-ζ polarized Slater-type basis QZ4P optimized for ZORA calculations (ZORA/QZ4P). The quadrupole coupling constants ($C_Q$), which are linearly dependent on the EFG, can be calculated accordingly. These spin polarized calculations predict the ground state as an antiferromagnetically coupled singlet state, and the high-spin state (septet) is found to be 4.4 kcal/mol higher in energy. Orbital analysis shows that the unpaired spin density is localized on the manganese centers as a $d^3$−$d^3$ configuration. The computed singlet−septet energy difference corresponds to an exchange coupling constant of −128 cm$^{-1}$ using the approach by the Ruiz group for strong bonding molecules,[41,42] on the order of the experimentally measured $J$-value and consistent with the tendency of BS-DFT to overestimate it.[43] The Heisenberg exchange constant is also evaluated by the approach proposed by L. Noodleman[32] for weakly bonded systems and the method proposed by M. Nishino el. al. for all bonding interactions[44] (see details in the Supporting Information). The deviation from the experimental value is larger, which is consistent with the previous report.[42] The quadrupole coupling constant tends to be more accurately computed, and $C_Q$ is given by

$$C_Q = q_{zz}\left[\frac{e^2}{a_0^3 h}\right]Q \quad (1)$$

$$= q_{zz} \cdot 77.5384 \text{ MHz} \quad (2)$$

Here, $Q$ is the $^{55}$Mn quadrupole moment and $q_{zz}$ is defined as the largest magnitude of the computed field gradient tensor. The asymmetry parameter has its usual definition, $\eta_Q = (q_{xx} - q_{yy})/q_{zz}$ where $|q_{xx}| \le |q_{yy}| \le |q_{zz}|$. The units for $q_{zz}$ are atomic units, and the factor of 77.5384 MHz can be computed if the atomic constants are expressed in cgs units and the value of $Q$ is given as $0.330 \times 10^{-24}$ cm$^2$.[45] The calculated $C_Q$ for the broken-symmetry state is 23.4 MHz with $\eta_Q$ = 0.682, in good agreement with the experimentally determined values.

Electron nuclear double resonance (ENDOR) spectroscopy has been used previously to determine $C_Q$[46] for the Mn(IV) centers in tetrakisbipyridine (+40 MHz)[47] and phenanthroline (+55 MHz)[48] ligated mixed-valent Mn(III,IV) $\mu$-oxido bridged dimers. These

species each possess a *cis*-$N_4O_2$ type coordination environment for the Mn centers, in contrast to the *cis*-$N_2O_4$ donor set for **1**. Perhaps the anionic phenoxy ligand in the axial position of the salpn complex reduces the oblate character of the Mn(IV) electron cloud compared to the $N_4O_2$ compounds, or maybe these changes in the EFG are due to reduction at the adjacent Mn. A detailed theoretical treatment is underway to understand more precisely such effects on the EFG.

These first solid-state $^{55}$Mn NMR data of an antiferromagnetically coupled $S = 0$ species illustrate the promise of this technique in the exploration of models of the OEC and perhaps even the $Mn_4Ca$ cluster itself. The extrapolation of these results to PS(II) needs more calibration and tuning with a variety of ligand geometries and oxidation states (IV/IV and III/III) to gain confidence in our ability to predict the likely states to be found in the OEC. Further, the dilution of the OEC associated with the higher molecular weight of PS(II) presents the challenge of a significant loss in sensitivity. The latter difficulty could be overcome by employing a dynamic nuclear polarization (DNP) experiment in combination with the methods outlined above. Overall, these results suggest that the cryogenic solid-state NMR experiment illustrated here in coupling with theory has sufficient sensitivity to characterize the NMR parameters of antiferromagnetically coupled metal centers in metalloproteins with the state $S = 0$.

**Acknowledgment.** This research was carried out in the Environmental Molecular Sciences Laboratory (a national scientific user facility sponsored by the U.S. Department of Energy's Office of Biological and Environmental Research) located at Pacific Northwest National Laboratory and operated for the DOE by Battelle. P.D.E. would like to thank the Biological Sciences Division for its partial support of this effort. P.Y. and A.S.L. acknowledge partial support from the EMSL for this work through its intramural program. Support to R.D.B. was provided by NIH GM-48242. R.D.B. thanks D. W. Randall (Andrews University) for useful discussions.

**Supporting Information Available:** The evaluation of the Heisenberg exchange constant using various methods and the calculated molecular coordinates. This material is available free of charge via the Internet at http://pubs.acs.org.

## References

(1) Pecoraro, V. L.; Baldwin, M. J.; Caudle, M. T.; Hsieh, W. Y.; Law, N. A. *Pure Appl. Chem.* **1998**, *70*, 925–929.
(2) Pecoraro, V. L.; Hsieh, W. Y. *Inorg. Chem.* **2008**, *47*, 1765–1778.
(3) Yachandra, V. K.; Sauer, K.; Klein, M. P. *Chem. Rev.* **1996**, *96*, 2927–2950.
(4) Tommos, C.; Babcock, G. T. *Acc. Chem. Res.* **1998**, *31*, 18–25.
(5) Nocera, D. G. *Inorg. Chem.* **2009**, *48*, 10001–10017.
(6) Barber, J. *Chem. Soc. Rev.* **2009**, *38*, 185–196.
(7) Ferreira, K. N.; Iverson, T. M.; Maghlaoui, K.; Barber, J.; Iwata, S. *Science* **2004**, *303*, 1831–1838.
(8) Peloquin, J. M.; Campbell, K. A.; Randall, D. W.; Evanchik, M. A.; Pecoraro, V. L.; Armstrong, W. H.; Britt, R. D. *J. Am. Chem. Soc.* **2000**, *122*, 10926–10942.
(9) Yano, J.; Yachandra, V. K. *Inorg. Chem.* **2008**, *47*, 1711–1726.
(10) Kulik, L. V.; Epel, B.; Lubitz, W.; Messinger, J. *J. Am. Chem. Soc.* **2007**, *129*, 13421–13435.
(11) Yano, J.; Kern, J.; Sauer, K.; Latimer, M. J.; Pushkar, Y.; Biesiadka, J.; Loll, B.; Saenger, W.; Messinger, J.; Zouni, A.; Yachandra, V. K. *Science* **2006**, *314*, 821–825.
(12) Sproviero, E. M.; McEvoy, J. P.; Gascon, J. A.; Brudvig, G. W.; Batista, V. S. *Photosynth. Res.* **2008**, *97*, 91–114.
(13) Pantazis, D. A.; Orio, M.; Petrenko, T.; Zein, S.; Lubitz, W.; Messinger, J.; Neese, F. *PCCP Phys. Chem. Chem. Phys.* **2009**, *11*, 6788–6798.
(14) Kok, B.; Forbush, B.; Mcgloin, M. *Photochem. Photobiol.* **1970**, *11*, 457-&.
(15) Lipton, A. S.; Heck, R. W.; Ellis, P. D. *J. Am. Chem. Soc.* **2004**, *126*, 4735–4739.
(16) Lipton, A. S.; Ellis, P. D. *J. Am. Chem. Soc.* **2007**, *129*, 9192–9200.
(17) Lipton, A. S.; Heck, R. W.; Staeheli, G. R.; Valiev, M.; De Jong, W. A.; Ellis, P. D. *J. Am. Chem. Soc.* **2008**, *130*, 6224–6230.
(18) Lipton, A. S.; Heck, R. W.; Hernick, M.; Fierke, C. A.; Ellis, P. D. *J. Am. Chem. Soc.* **2008**, *130*, 12671–12679.
(19) Lipton, A. S.; Heck, R. W.; de Jong, W. A.; Gao, A. R.; Wu, X. J.; Roehrich, A.; Harbison, G. S.; Ellis, P. D. *J. Am. Chem. Soc.* **2009**, *131*, 13992–13999.
(20) Larson, E.; Lah, M. S.; Li, X.; Bonadies, J. A.; Pecoraro, V. L. *Inorg. Chem.* **1992**, *31*, 373–378.
(21) Gohdes, J. W.; Armstrong, W. H. *Inorg. Chem.* **1992**, *31*, 368–373.
(22) Larsen, F. H.; Jakobsen, H. J.; Ellis, P. D.; Nielsen, N. C. *J. Phys. Chem. A* **1997**, *101*, 8597–8606.
(23) Larsen, F. H.; Lipton, A. S.; Jakobsen, H. J.; Nielsen, N. C.; Ellis, P. D. *J. Am. Chem. Soc.* **1999**, *121*, 3783–3784.
(24) Lipton, A. S.; Sears, J. A.; Ellis, P. D. *J. Magn. Reson.* **2001**, *151*, 48–59.
(25) Using $H = -2J_{12}S_1 \cdot S_2$.
(26) Baldwin, M. J.; Stemmler, T. L.; Riggs-Gelasco, P. J.; Kirk, M. L.; Penner-Hahn, J. E.; Pecoraro, V. L. *J. Am. Chem. Soc.* **1994**, *116*, 11349–11356.
(27) Moncho, S.; Autschbach, J. *J. Chem. Theory Comput.* **2010**, *6*, 223–234.
(28) Autschbach, J. *Struct. Bonding (Berlin)* **2004**, *112*, 63–82.
(29) Autschbach, J.; Ziegler, T. *Coord. Chem. Rev.* **2003**, *238*, 83–126.
(30) Autschbach, J.; Ziegler, T. *J. Chem. Phys.* **2000**, *113*, 9410–9418.
(31) Krykunov, M.; Ziegler, T.; Van Lenthe, E. *Int. J. Quantum Chem.* **2009**, *109*, 1676–1683.
(32) Noodleman, L. *J. Chem. Phys.* **1981**, *74*, 5737–5743.
(33) Noodleman, L.; Davidson, E. R. *Chem. Phys.* **1986**, *109*, 131–143.
(34) te Velde, G.; Bickelhaupt, F. M.; Baerends, E. J.; Guerra, C. F.; van Gisbergen, S. J. A.; Snijders, J. G.; Ziegler, T. *J. Comput. Chem.* **2001**, *22*, 931–967.
(35) Guerra, C. F.; Snijders, J. G.; te Velde, G.; Baerends, E. J. *Theor. Chem. Acc.* **1998**, *99*, 391–403.
(36) *ADF2009.01.*; SCM, Theoretical Chemistry, Vrije Universiteit: Amsterdam, The Netherlands, 2009.
(37) van Lenthe, E.; Baerends, E. J.; Snijders, J. G. *J. Chem. Phys.* **1993**, *99*, 4597–4610.
(38) van Lenthe, E.; Ehlers, A.; Baerends, E. J. *J. Chem. Phys.* **1999**, *110*, 8943–8953.
(39) Perdew, J. P.; Burke, K.; Ernzerhof, M. *Phys. Rev. Lett.* **1996**, *77*, 3865–3868.
(40) Perdew, J. P.; Burke, K.; Ernzerhof, M. *Phys. Rev. Lett.* **1997**, *78*, 1396–1396.
(41) Ruiz, E.; Cano, J.; Alvarez, S.; Alemany, P. *J. Comput. Chem.* **1999**, *20*, 1391–1400.
(42) Rudberg, E.; Salek, P.; Rinkevicius, Z.; Agren, H. *J. Chem. Theory Comput.* **2006**, *2*, 981–989.
(43) Sinnecker, S.; Neese, F.; Noodleman, L.; Lubitz, W. *J. Am. Chem. Soc.* **2004**, *126*, 2613–2622.
(44) Nishino, M.; Yamanaka, S.; Yoshioka, Y.; Yamaguchi, K. *J. Phys. Chem. A* **1997**, *101*, 705–712.
(45) Pyykko, P. *Mol. Phys.* **2001**, *99*, 1617–1629.
(46) $C_Q$ is related to the principal quadrupole tensor element $P_{||}$ by the factor $4I(2I-1)/3$.
(47) Randall, D. W.; Sturgeon, B. E.; Ball, J. A.; Lorigan, G. A.; Chan, M. K.; Klein, M. P.; Armstrong, W. H.; Britt, R. D. *J. Am. Chem. Soc.* **1995**, *117*, 11780–9.
(48) Randall, D. W.; Chan, M. K.; Armstrong, W. H.; Britt, R. D. *Mol. Phys.* **1998**, *95*, 1283–1294.

JA1054252